SURFACE AND INTERFACE ANALYSIS
Surf. Interface Anal. 2005; **37**: 895–900
Published online in Wiley InterScience (www.interscience.wiley.com). DOI: 10.1002/sia.2107

SIA

A new examination of secondary electron yield data

Yinghong Lin[1] and David C. Joy[1,2]*

[1] University of Tennessee, Knoxville, TN 37996-0840, USA
[2] Oak Ridge National Laboratory, Oak Ridge, TN 37831-6064, USA

Received 8 November 2004; Revised 22 March 2005; Accepted 22 March 2005

A new and thorough examination of secondary electron (SE) yield as a function of primary energy (E_{PE}) and atomic number Z for the 44 elements in the database[1] is made. The principles of the semiempirical universal law for the SE yield are described and a template for Monte Carlo (MC) simulation is produced accordingly. Both universal curve fitting and MC simulation are made for the 44 elements. The resulted maximum SE yield δ^m, corresponding primary energy E_{PE}^m, SE excitation energy ε, and effective escape depth λ are tabulated and plotted as a function of atomic number Z. It is found that similarities exist in the profiles of ε and λ, δ^m and E_{PE}^m, and all of these parameters seem to have characteristics associated with atomic shell filling.

KEYWORDS: secondary electron yield; SE excitation energy; SE effective escape depth; SE universal curve; atomic shell filling

INTRODUCTION

Secondary electrons (SEs) are those that are emitted from a target as the result of irradiation by an energetic beam of electrons, protons, or ions, and which have a kinetic energy of 50 eV or less. SEs are the basis of the most widely used imaging mode in the scanning electron microscope,[2] and they also play important roles in other areas as diverse as particle accelerators, plasma TV display, the performance of high-voltage insulators, and the stability of space satellites in the solar wind.[3,4]

The parameter describing SE emission is the yield δ, which is defined as the number of SEs produced by each incident particle which, for the purposes of this paper, will be assumed to be a primary electron (PE), referred to as an incident electron with energy E_{PE}. The information that is required in any study dealing with the SE emission is how the yield δ varies with the incident energy of the electrons and with the atomic number Z of the target. Consequently, in the century since SEs were first described, much work has been performed to determine δ as a function of E_{PE} and Z for elements and materials of interest. Such yield curves are not only useful for providing specific data values for investigative purposes but also for providing a way of testing and calibrating Monte Carlo (MC)[5] simulations of electron-solid interactions and SE generation.

A compilation of SE yield profiles for incident electron energies up to 50 keV, presently covering 51 elements and 42 compounds, and representing over 80 years of published data from more than one hundred different groups of authors is available for download from http://pciserver.bio.utk.edu[1] and also from http://www.napchan.com/bse/index.htm or directly from the authors. An examination of this data is discouraging, because it is evident that even for common elements (such as aluminum or gold) for which there are often a dozen or more independent sets of data available, the level of agreement is rarely better than 25% and often shows relative divergences of 100% or more. The result of this situation is that anyone seeking yield data to explain an observation or to validate a model can usually find multiple values spanning a large enough range to support or disprove any assertion.

The goal of this paper is to try and improve this situation by using the well-established concept of a 'universal yield curve of SE production'[2,6,7] as a tool with which to examine these experimental results, to identify and correct the possible sources of error in the data, and then to generate an optimized SE yield profile for each element for which an adequate supply of experimental results is available. We believe that these synthesized yield profiles provide much more reliable data on SE emission for predictive or test purposes than the corresponding 'raw' published values. As an additional benefit, the magnitude of the four parameters discussed in the following text, which appear in the analytical expression for the yield curve, can be examined as a function of the atomic number Z to provide additional insights into the way in which SE emission depends on the target material.

THE SEMIEMPIRICAL UNIVERSAL LAW

The SE emission rate $\delta(E_{PE})$ depends on the rate $n(z, E)$ at which SEs are generated as a function of depth z.[2,6–8]

$$n(z, E) = -\frac{1}{\varepsilon} \cdot \frac{dE}{ds} \tag{1}$$

where s is the path length measured along the electron trajectory, and dE/ds is the stopping power of the incident electron, i.e. the rate at which the incident electron transfers energy to the material through which it is moving,[9] and

*Correspondence to: David C. Joy, Room 232, SERF, University of Tennessee, Knoxville, TN 37996-0840, USA. E-mail: djoy@utk.edu

ε is the effective energy required to produce an SE. The probability $p(z)$ that a generated SE will escape back to the incident surface is then[6,7,10–12]

$$p(z) = K \exp\left(-\frac{z}{\lambda}\right) \tag{2}$$

where $K = 0.5$ assuming that SE are scattered symmetrically in specimen. λ is the effective SE escape depth.

Thus,

$$\delta(E_{\mathrm{PE}}) = \int n(z, E) \cdot p(z) \cdot \mathrm{d}z \tag{3}$$

For all materials for which data has been obtained (http://pciserver.bio.utk.edu and http://www.napchan.com/bse/index.htm), the general yield curve of $\delta(E_{\mathrm{PE}})$ with E_{PE} has the shape shown in Fig. 1. The yield rises from zero at the lowest energies, reaches a maximum δ^{m} at some energy $E_{\mathrm{PE}}^{\mathrm{m}}$ with $\delta^{\mathrm{m}} \approx 1$, $E_{\mathrm{PE}}^{\mathrm{m}} \approx 1$ keV, and then falls monotonically at about $1/E_{\mathrm{PE}}$ at higher energies.[2,7]

Because all experimental yield curves have the same generic shape, there have been many attempts to provide an analytical description of the profile. The simplest approach would be to assume a constant stopping power,[6,7,13] then

$$-\frac{\mathrm{d}E}{\mathrm{d}s} = \frac{E_{\mathrm{PE}}}{R} \tag{4}$$

where R is the range or penetration depth of the incident electron. Equation (3) then gives

$$\delta = 0.5\frac{E_{\mathrm{PE}}}{\varepsilon} \cdot \frac{\lambda}{R}(1 - \mathrm{e}^{-R/\lambda}) \tag{5}$$

Other simple approximations describing the stopping power[2,13] give similar results to Eqn (5).

The electron range R as a function of energy E_{PE} is

$$R = \frac{B}{\rho} \cdot (E_{\mathrm{PE}})^n \tag{6}$$

where $n = 1.67$ according to Lane and Zaffarano,[14] $B = 76$ nm for E_{PE} in kilo electron volts, and ρ is the density of the target material in grams per cubic centimeter.

Dionne[15] calculated the maximum SE yield δ^{m} and the corresponding primary energy $E_{\mathrm{PE}}^{\mathrm{m}}$ by differentiating an equation similar to (5) and showed that when $\delta = \delta^{\mathrm{m}}$,

$$\frac{R}{\lambda} = \left(1 - \frac{1}{n}\right)(\mathrm{e}^{R/\lambda} - 1) \tag{7}$$

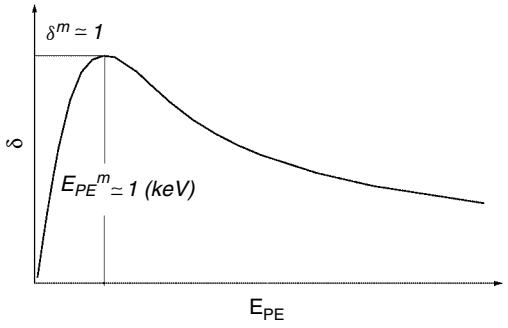

Figure 1. Schematic profile of SE yields δ as a function of primary energy E_{PE}.

So for $n = 1.67$,

$$R = 1.614\lambda \tag{8}$$

Substitution of (8) into (6) gives,

$$E_{\mathrm{PE}}^{\mathrm{m}} \approx 1.33\left(\frac{\rho \cdot \lambda}{B}\right)^{0.60} \tag{9}$$

Substitution of (9) into (5) gives

$$\delta^{\mathrm{m}} \approx \frac{0.33}{\varepsilon}\left(\frac{\rho \cdot \lambda}{B}\right)^{0.60} \tag{10}$$

It has been proved that $\delta^{\mathrm{m}}/E_{\mathrm{PE}}^{\mathrm{m}}$ is a constant of material characteristics.[5,16] In our calculation,

$$\frac{\delta^{\mathrm{m}}}{E_{\mathrm{PE}}^{\mathrm{m}}} = \frac{0.248}{\varepsilon} \tag{11}$$

Because ε and λ are not known in general, they must be eliminated from the expression. This can be done by combining Eqns (5), (6), (9), and (10), which gives $\delta/\delta^{\mathrm{m}}$ as a function of $E_{\mathrm{PE}}/E_{\mathrm{PE}}^{\mathrm{m}}$ that is independent of the material:

$$\frac{\delta}{\delta^{\mathrm{m}}} = 1.28\left(\frac{E_{\mathrm{PE}}}{E_{\mathrm{PE}}^{\mathrm{m}}}\right)^{-0.67}\left(1 - \exp\left(-1.614\left(\frac{E_{\mathrm{PE}}}{E_{\mathrm{PE}}^{\mathrm{m}}}\right)^{1.67}\right)\right) \tag{12}$$

This result usually referred to as 'the universal law for SE yield' provides a conventional description of the phenomena of SE emission. Other forms of this law were given by many other authors.[2,7,15,17–19]

EXAMINING THE DATABASE

The experimental SE yield values in the database represent the work of more than 100 authors spread over a time period of nearly 100 years. Consequently, the quality of the data varies greatly and, except for those examples where only a single set of measurements is available, there are always significant variations between yield values at a given energy. These differences may be the result of the sample preparation, the experimental arrangement, or poor laboratory technique. But in any case, the goal is to extract from these assorted data sets the best estimate of the SE yield $\delta(E_{\mathrm{PE}})$ *versus* energy E_{PE}. The universal law of SE yield provides the tool with which to do this.

Figure 2 shows the available $\delta(E_{\mathrm{PE}})$ data for aluminum. A total of 13 separate measurements is plotted. It can be seen that although all of the data agree that the maximum SE yield δ^{m} occurs at energy of 400 eV, the measured value of δ^{m} is variously quoted from 0.5 to 3.3. The question is, therefore, how relative numerical values of the yield *versus* energy can be obtained, given the often enormous spread of experimental values.

For the purposes of computing an SE yield curve against energy, given values of $E_{\mathrm{PE}}^{\mathrm{m}}$ and δ^{m} or, correspondingly, ε and λ, a simple MC extension of the model of Salow[6] or Dekker[7] can be used.[20] Instead of assuming a constant stopping power, a modified Bethe model for stopping power given by Joy and Luo is used in the calculation,[5,21,22]

$$\frac{\mathrm{d}E}{\mathrm{d}s} = -78\,500 * \frac{Z}{AE} * \ln\left(\frac{1.166(E + 0.85J)}{J}\right) \tag{13}$$

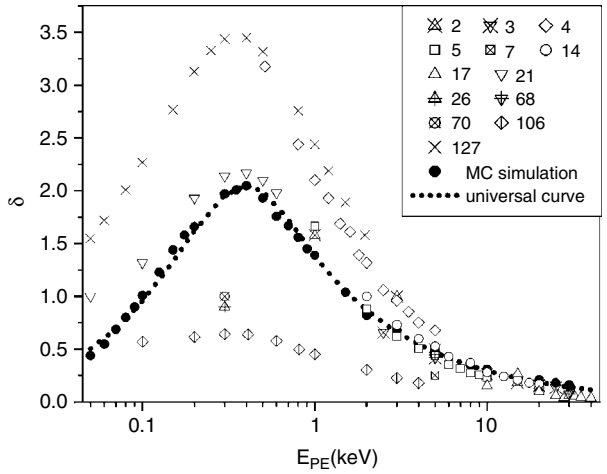

Figure 2. SE yield δ for Al. Symbols other than dots represent data from the database. Numbers in the legend correspond to the references cited. $\lambda = 1.7$ nm, $\varepsilon = 23$ eV are for the MC simulation. $E_{PE}^{m} = 0.4$ keV and $\delta^{m} = 2.5$ are for the universal curve calculation.

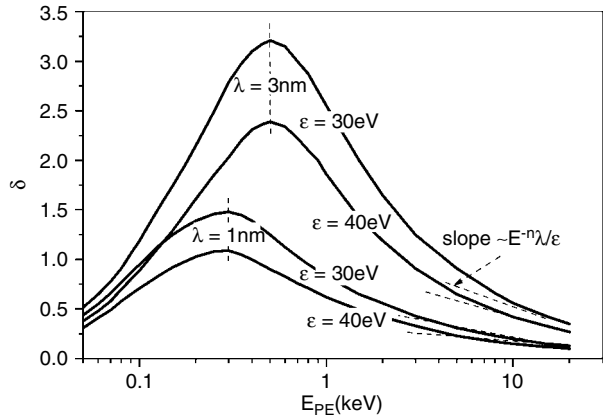

Figure 3. Template for MC simulation of SE yield profile. SE excitation energy ε and effective escape depth λ are two key parameters.

which incorporates more detailed information like atomic number Z, atomic weight A, and mean ionization potential J of the target material. The electron scattering is treated using a modified plural scattering model and a corrected Rutherford cross section. In a modern PC, this computation can be carried out very rapidly for energies between 0.1 and 20 keV and specified ε and λ values, and provides a completed yield curve that combines the essential concept of the universal law with the added benefit of an enhanced physical model. Under most circumstances, the agreement between the universal curve of Eqn (5) and the MC simulation computed for the ε and λ values is close. Either representation of the yield could therefore be employed. For convenience, in the subsequent discussion, both versions will be displayed, as shown in Fig. 2.

Figure 3 shows yield curves calculated using the MC model discussed in the preceding text, assuming the sample to be aluminum but varying the parameters ε and λ. For example, the two profiles for which $\lambda = 1$ nm, have closely similar shapes with a maximum yield occurring at 0.3 keV. Similarly, the two profiles for which $\lambda = 3$ nm also show δ^{m} occurring at the same energy (0.5 keV). This is of course consistent with Eqn (8). Changing the value of λ, while keeping ε constant, leads to a shift in E_{PE}^{m} as well as a change in the value of δ^{m}. If we treat the data of Fig. 3 as a template, then it is clear that those experimental data sets that show smaller E_{PE}^{m} represent smaller λ values. Smaller or larger values of δ^{m} can similarly be correlated with higher or lower values of ε. Note also that at high energies ($E_{PE} \gg E_{PE}^{m}$), the yield δ is directly dependent on $\left(\frac{\lambda}{\varepsilon}\right) E_{PE}^{1-n}$ according to Eqns (5) and (6) and thus has a slope of about $\left(\frac{\lambda}{\varepsilon}\right) E_{PE}^{-n}$.

Our procedure has therefore been to empirically fit the available yield curves from different authors for a given material using the results of Eqns (8), (9), and (10) to estimate initial ε and λ values, which are then incorporated into the MC simulation. The fit of this prediction with the various experimental results is then optimized to obtain final values of ε and λ and hence of δ^{m} and E_{PE}^{m}. By focusing on ε, λ, and hence the shape of the yield curve, rather than on the actual values of δ, a more reliable assessment of the data can be made.

RESULTS AND DISCUSSION

The database contains results for 51 elements. Most of these have two or more independent sets of data, and 19 have five or more. In a few cases, the data is very sparse and consists only of E_{PE}^{m} and δ^{m} values, and no attempt has been made to analyze this data. For the 44 remaining examples, the procedures discussed above can be used to obtain 'best practice' values for ε and λ and then to derive the corresponding SE yield curve to provide $\delta(E_{PE})$ values at energies for which no experimental data is available.

The Al data of Fig. 2 and the Ti data of Fig. 4 exemplify the problems discussed in the preceding text. The multiple data sets show significant differences in $\delta(E_{PE})$ and δ^{m} values. However, for both elements, the E_{PE}^{m} values are in good agreement, and in both cases, the variations of $\delta(E_{PE})$ with E_{PE}

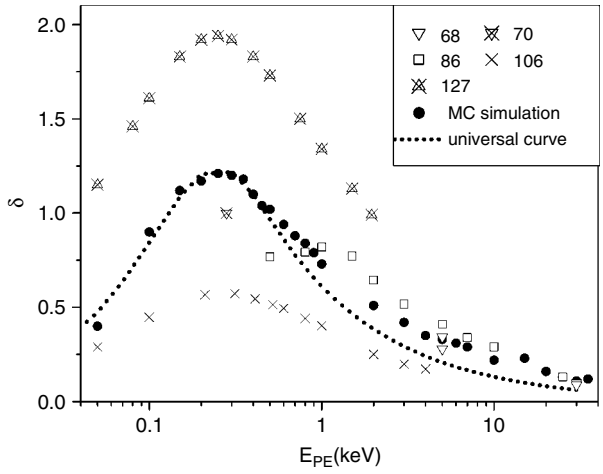

Figure 4. SE yield δ for Ti. Symbols other than dots represent data from the database. Numbers in the legend correspond to the references cited. $\lambda = 0.5$ nm and $\varepsilon = 25$ eV are for the MC simulation. $E_{PE}^{m} = 0.25$ keV and $\delta^{m} = 1.21$ are for the universal curve calculation.

at high energies are very similar. From these observations, we can deduce most probable values for λ and λ/ε. Inserting these parameters into Eqn (5) or into the MC model then generates yield curves, which are clearly in good agreement with the overall shape and magnitude of the yield profile and which provide a quality estimate of δ at any energy.

The same procedure has been applied to all 44 of the useful data sheets to produce ε and λ values and the corresponding yield profiles. The yield curves can then be generated by downloading the MC program from http://pciserver.bio.utk.edu/metrology and inserting the appropriate values or by applying Eqn (5) and using a suitable range equation.

The optimum values of ε and λ for each element are tabulated in Table 1. We believe that these values and the yield curves generated by using them represent the

Table 1. Data for elements from Monte Carlo simulation

Element	Z	ε (eV)	λ (nm)	$\frac{\varepsilon}{\lambda}$	R (nm)	$\frac{R}{\lambda}$	δ^{m}	E_{PE}^{m} (keV)	$\frac{\delta^{m}}{E_{PE}^{m}}$	δ at 20 keV	δ at 2 keV	ϕ^{b} (eV)
Li	3	45	2.0	2.25	8	4.00	0.59	0.15	3.93	0.03	0.14	2.9
Be	4	70	1.0	7.0	3	3.00	0.55	0.20	2.75	0.02	0.11	4.98
B	5	40	1.0	4.0	3	3.00	1.05	0.24	4.38	0.06	0.32	4.45
C	6	80	2.5	3.2	7	2.80	1.06	0.40	2.65	0.08	0.37	5
Mg	12	50	1.3	3.85	6	4.62	0.80	0.24	3.33	0.07	0.32	3.66
Al	13	32	1.7	1.88	10	4.71	2.00	0.40	5.00	0.19	0.84	4.28
Si[a]	14	90	2.7	3.33	12	4.44	0.89	0.45	1.98	0.08	0.44	4.85
K	19	100	2.0	5.0	16	8.00	0.27	0.22	1.23	0.02	0.12	2.3
Ca	20	40	0.5	8.0	5	10.0	0.33	0.15	2.20	0.05	0.14	2.87
Sc	21	30	0.5	6.0	4	8.00	0.76	0.20	3.80	0.11	0.3	3.5
Ti	22	25	0.5	5.0	4	8.00	1.21	0.25	4.84	0.16	0.51	4.33
Cr	24	47	1.2	3.92	6	6.67	1.80	0.60	3.00	0.27	1.01	4.5
Fe	26	45	0.6	7.5	4	6.67	1.15	0.35	3.29	0.15	0.58	4.5
Ni	28	65	1.0	6.5	5	5.00	1.19	0.50	2.38	0.20	0.7	5.15
Cu	29	35	0.6	5.83	4	6.67	1.53	0.40	3.83	0.24	0.83	4.65
Zn	30	120	2.5	4.80	11	4.40	1.03	0.70	1.47	0.19	0.72	4.33
Ga	31	90	1.5	6.00	8	5.33	0.78	0.45	1.73	0.13	0.48	4.2
Ge	32	50	1.0	5.00	8	8.00	1.00	0.40	2.50	0.15	0.53	5
Se	34	28	0.5	5.60	5	10.0	0.86	0.25	3.44	0.13	0.44	5.9
Sr	38	50	1.0	5.00	11	11.0	0.49	0.25	1.96	0.09	0.27	2.59
Y	39	60	1.0	6.00	11	11.0	0.65	0.40	1.63	0.12	0.35	3.1
Zr	40	35	0.5	7.00	5	10.0	0.83	0.30	2.77	0.14	0.51	4.05
Nb	41	20	0.3	6.67	3	10.0	1.16	0.25	4.64	0.25	0.65	4.3
Mo	42	60	1.0	6.00	7	7.00	1.14	0.50	2.28	0.25	0.74	4.6
Pd	46	55	1.0	5.50	7	7.00	1.41	0.55	2.56	0.32	0.94	5.12
Ag	47	50	1.0	5.00	9	9.00	1.43	0.60	2.38	0.31	0.96	4.26
Cd	48	70	1.5	4.67	13	8.67	1.16	0.65	1.78	0.26	0.82	4.22
In	49	40	1.0	4.00	11	11.0	1.29	0.50	2.58	0.27	0.81	4.12
Sn	50	43	1.0	4.30	10	11.0	1.12	0.50	2.24	0.27	0.77	4.42
Sb	51	80	2.5	3.20	16	7.60	1.16	0.70	1.66	0.25	0.89	4.7
Te	52	50	1.0	5.00	9	9.00	0.84	0.35	2.40	0.19	0.5	4.95
Cs	55	60	3.5	1.71	38	10.9	0.72	0.40	1.80	0.16	0.46	2.14
Ba	56	53	2.0	2.65	24	12.0	0.83	0.45	1.84	0.19	0.53	2.7
La	57	54	1.0	5.40	15	15.0	0.72	0.50	1.44	0.15	0.44	3.5
Hf	72	45	1.0	4.50	11	11.0	1.39	0.60	2.32	0.37	1.07	3.9
Ta	73	60	0.7	8.57	9	12.9	0.93	0.65	1.43	0.37	0.66	4.25
W	74	20	0.2	10.0	3	15.0	1.06	0.25	4.24	0.31	0.71	4.55
Re	75	50	0.6	8.33	7	11.7	1.20	0.60	2.00	0.34	0.88	4.96
Pt	78	30	0.5	6.00	6	12.0	1.69	0.55	3.07	0.47	1.22	5.65
Au	79	35	0.5	7.00	7	12.0	1.28	0.50	2.56	0.37	0.94	5.1
Hg	80	48	1.0	4.80	14	14.0	1.23	0.70	1.76	0.36	0.98	4.49
Tl	81	40	0.8	5.00	11	13.8	1.09	0.50	2.18	0.3	0.76	3.84
Pb	82	40	0.8	5.00	12	15.0	1.06	0.50	2.12	0.28	0.72	4.25
Bi	83	80	2.0	4.00	20	10.0	0.98	0.70	1.40	0.31	0.79	4.22

[a] Silicon crystal.

[b] Data in Ref. 23.

most reliable estimate of SE emission data that is presently available for modeling and interpretive purposes. Table 1 also lists δ^m, E_{PE}^m, and δ at 2 and 20 keV for each of the 44 elements analyzed together with their work function ϕ.[23] A plot of λ, ε, δ^m, E_{PE}^m or any of the data sets as a function of the atomic number Z of the target shows large, seemingly random, fluctuations with no evidence of trends (e.g. Figs 5 and 6). However, these plots have a generally similar form,

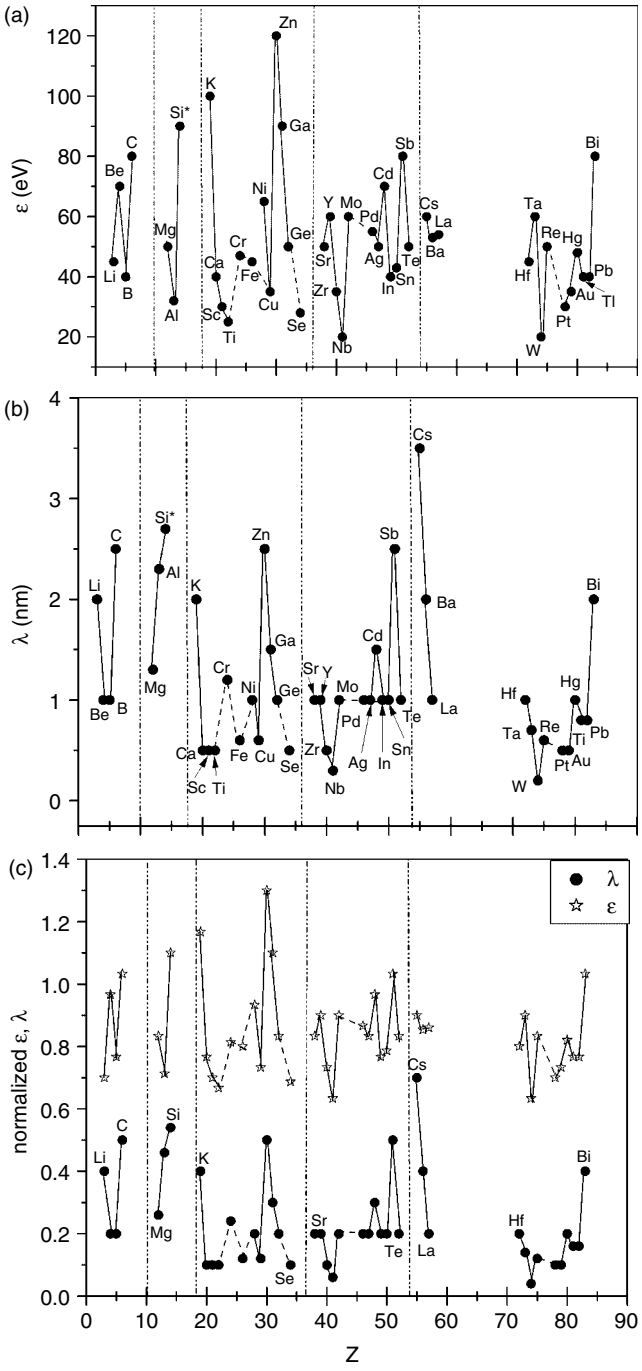

Figure 5. SE excitation energy ε (a) and effective escape depth λ (b) as functions of atomic number Z. (c) ε normalized to 150 eV and λ normalized to 5 nm show extremely similar shapes. Solid lines connect consecutive atomic number and dashed lines connect nonconsecutive atomic number. Normalized ε are shifted 0.5 up to make plot clear.

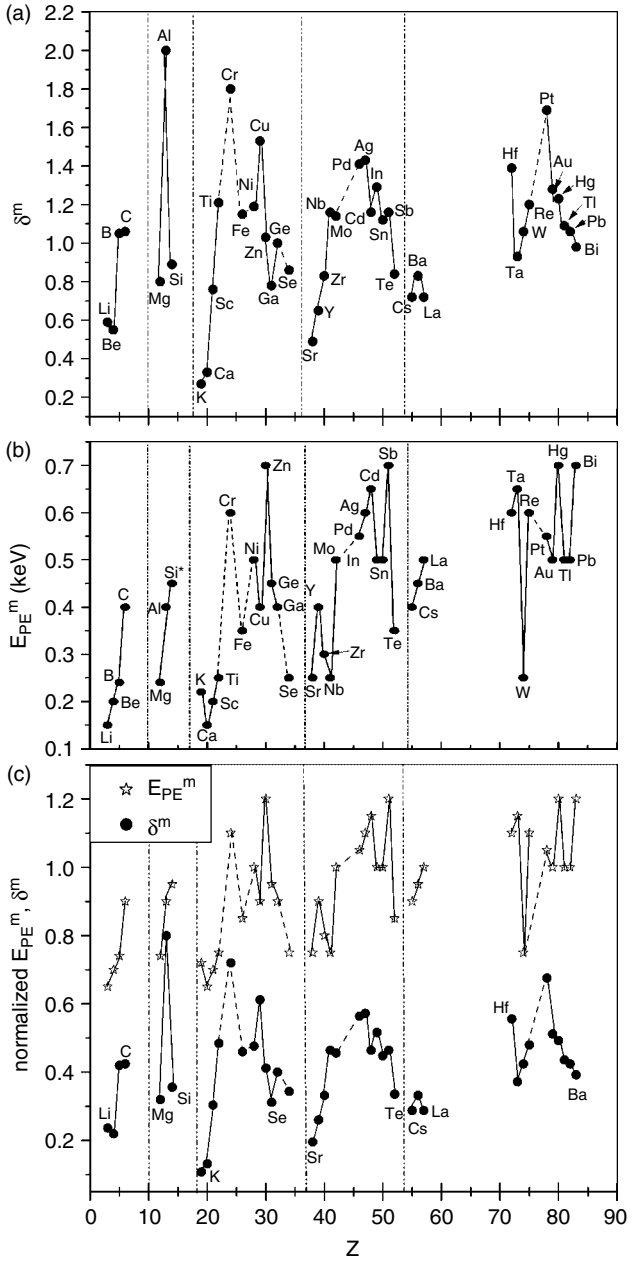

Figure 6. Maximum SE yield δ^m (a) and corresponding primary energy E_{PE}^m (b) as functions of atomic number Z. (c) E_{PE}^m normalized to 1 keV and δ^m normalized to 2.5 show recognizably similar shapes and shell filling effects. Solid lines connect consecutive atomic number and dashed lines connect nonconsecutive atomic number. Normalized E_{PE}^m are shifted 0.5 up to make plot clear.

and plotting λ and ε against Z (Fig. 5(c)) provides profiles that are strikingly similar in form. Plots of δ^m and E_{PE}^m (Fig. 6) also show recognizably similar profiles. Sternglass[24] conjectured that the form of δ^m *versus* Z variation revealed the effects of shell filling. It is evident that δ^m is lowest immediately above a filled shell boundary ($Z = 3$, $Z = 11$, $Z = 19$, etc.), and that all the tabulated parameters show similar characteristics. However, because the sequence of Z values is broken in many places, it is not possible to confirm this hypothesis, nor is there an obvious physical reason that might explain this behavior. A plot of the work function ϕ and the SE excitation

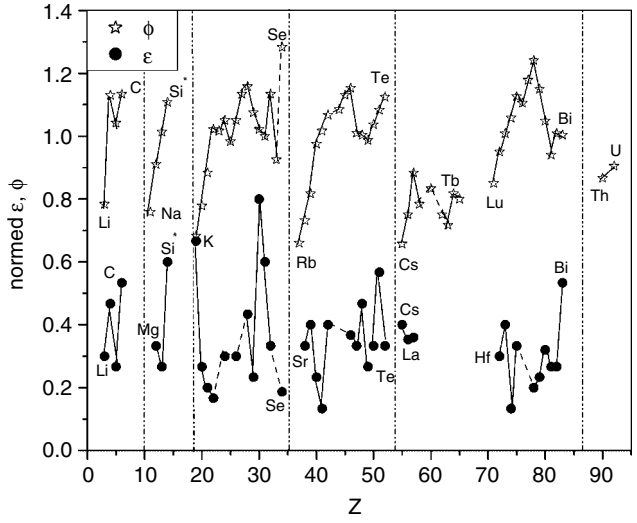

Figure 7. Work function ϕ normalized to 6 eV and SE excitation energy ε normalized to 150 eV as functions of atomic number Z. Normalized work functions are shifted 0.2 up to make plot clear. Solid lines connect consecutive atomic number and dashed lines connect nonconsecutive atomic number.

energy ε (Fig. 7) as a function of Z also shows that there is no simple relation between these two parameters, indicating that the SE yield variation with Z is not solely due to changes in the work function.

CONCLUSIONS

The use of a universal yield curve template provides a way to extract optimized data sets and modeling parameters from a confusing assembly of noisy, raw yield curves. The parameters that describe this data show a characteristic behavior which seems to represent the occurrence of shell filling. However, any conclusions about this must wait for additional experimental results to fill the conspicuous gaps that currently exist in the data. In addition, it is necessary to look at the behavior of the SE yield from compounds so as to identify the important factors that govern emission from mixture of atoms.

REFERENCES

1. Joy DC, UTK Metrology Group, http://pciserver.bio.utk.edu/metrology/download/E-solid/database.doc.. July 2004. 13 March. 2005. <http://pciserver.bio.utk.edu/metrology/download/E-solid/database.doc>.
2. Seiler H. *J. Appl. Phys.* 1983; **54**: R1.
3. Auday G, Guillot Ph, Galy J. *J. Appl. Phys.* 2000; **88**: 4871.
4. Hur MS, Lee JK, Kim HC, Kang BK. *IEEE Trans. Plasma Sci.* 2001; **29**: 861.
5. Joy DC. *Monte Carlo Modeling for Electron Microscopy and Microanalysis*. Oxford University Press: New York, Oxford, 1995; 134.
6. Salow H. *Phys. Z.* 1940; **41**: 434.
7. Dekker AJ. *Solid State Phys.*. Prentice-Hall: Englewood Cliffs, NJ, 1957; 418.
8. Bethe HA. *Phys. Rev.* 1941; **59**: 940.
9. Joy DC. *Scanning Microsc.* 1996; **10**: 653.
10. Bruining H. *Physics and Applications of Secondary Electron Emission*. Pergamon Press: London, 1954.
11. Hachenberg O, Brouer W. *Adv. Electron. Electron Phys.* 1959; **11**: 413.
12. Wittry DB, Kyser DF. *J. Appl. Phys.* 1965; **36**: 1387.
13. Young JR. *Phys. Rev.* 1956; **103**: 292.
14. Lane RO, Zaffarano DI. *Phys. Rev.* 1954; **94**: 960.
15. Dionne GF. *J. Appl. Phys.* 1975; **46**: 3347.
16. Ono S, Kanaya K. *J. Phys. D* 1979; **12**: 619.
17. Baroody EM. *Phys. Rev.* 1950; **78**: 780.
18. Jonker JLH. *Philips Res. Rep.* 1952; **7**: 1.
19. Dionne GF. *J. Appl. Phys.* 1973; **44**: 5361.
20. Joy DC. *J. Microsc.* 1987; **147**: 51.
21. Bethe HA. *Ann. Phys.* 1930; **5**: 325.
22. Joy DC, Luo S. *Scanning* 1989; **11**: 176.
23. Weast RC, Astle MJ, Beyer WH (eds). *CRC Handbook of Chemistry and Physics* (66th edn), CRC press: Boca Raton, FL, 1985–1986; E.
24. Sternglass EJ. *Phys. Rev.* 1950; **80**: 925.